

Supporting Information

**Co-designing growth factors for synthesis of (6, 5)-enriched
single-walled carbon nanotube horizontal array**

Junxiao Li^{1†}, Sizhe Lin^{1†}, Wei Liu¹, Changlong Li², Jiacheng Song², Zhiwei Liu², Yue Hu², Shuchen Zhang^{1*}

¹ State Key Laboratory of Precision and Intelligent Chemistry, Department of Materials Science and Engineering, School of Chemistry and Materials Science, University of Science and Technology of China, Hefei, Anhui 230026, China

² Key Laboratory of Carbon Materials of Zhejiang Province, College of Chemistry and Materials Engineering, Wenzhou University, Wenzhou 325000, P. R. China

*Corresponding Authors: S. Zhang

†These authors contributed equally to this work.



Figure S1. SEM images of quartz substrates after SWNT growth at 650 °C under fixed CO flow rate and varied Ar flow rates, thereby tuning the partial pressure of the carbon source. The catalysts used are **(a-d)** Co, **(e-h)** Co/Mo 3:1, **(i-l)** Co/Mo 2:1 and **(m-p)** Mo respectively.



Figure S2. SEM images of quartz substrates after SWNT growth at 700 °C under fixed CO flow rate and varied Ar flow rates, thereby tuning the partial pressure of the carbon source. The catalysts used are **(a-d)** Co, **(e-h)** Co/Mo 3:1, **(i-l)** Co/Mo 2:1 and **(m-p)** Mo respectively.



Figure S3. SEM images of quartz substrates after SWNT growth at 750 °C under fixed CO flow rate and varied Ar flow rates, thereby tuning the partial pressure of the carbon source. The catalysts used are **(a-d)** Co, **(e-h)** Co/Mo 3:1, **(i-l)** Co/Mo 2:1 and **(m-p)** Mo respectively.



Figure S4. SEM images of quartz substrates after SWNT growth at 800 °C under fixed CO flow rate and varied Ar flow rate, thereby tuning the partial pressure of the carbon source. The catalysts used are **(a-d)** Co, **(e-h)** Co/Mo 3:1, **(i-l)** Co/Mo 2:1 and **(m-p)** Mo respectively.

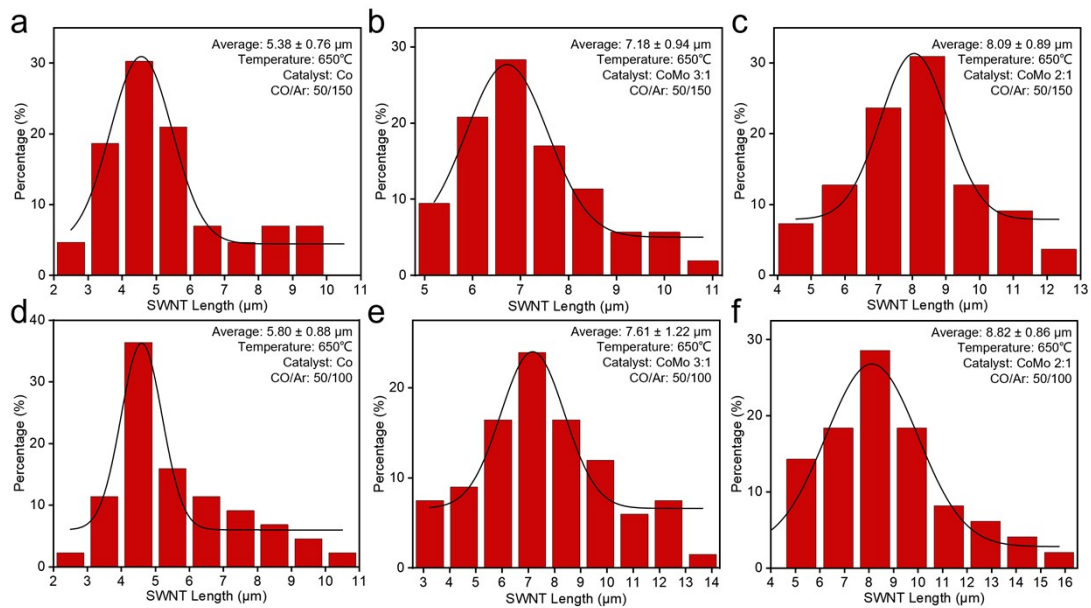


Figure S5. Length distributions of as-grown SWNTs at 650 °C under CO/Ar flow ratios of 50/150 and 50/100, grouped by catalytic active species, **(a, d)** Co, **(b, e)** Co/Mo 3:1 and **(c, f)** Co/Mo 2:1 respectively.

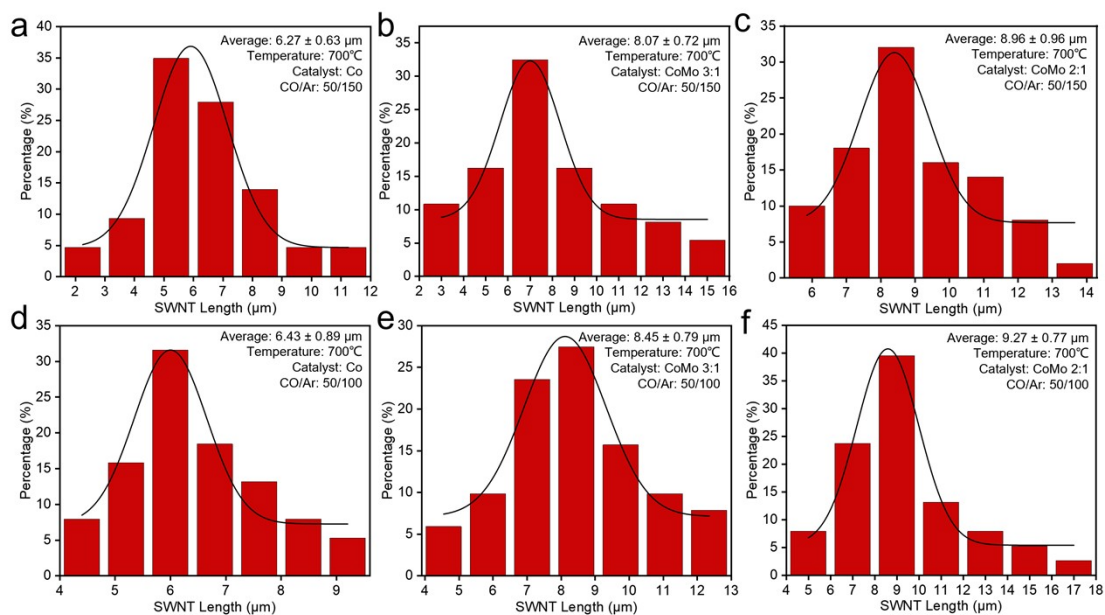


Figure S6. Length distributions of as-grown SWNTs at 700 °C under CO/Ar flow ratios of 50/150 and 50/100, grouped by catalytic active species, (a, d) Co, (b, e) Co/Mo 3:1 and (c, f) Co/Mo 2:1 respectively.

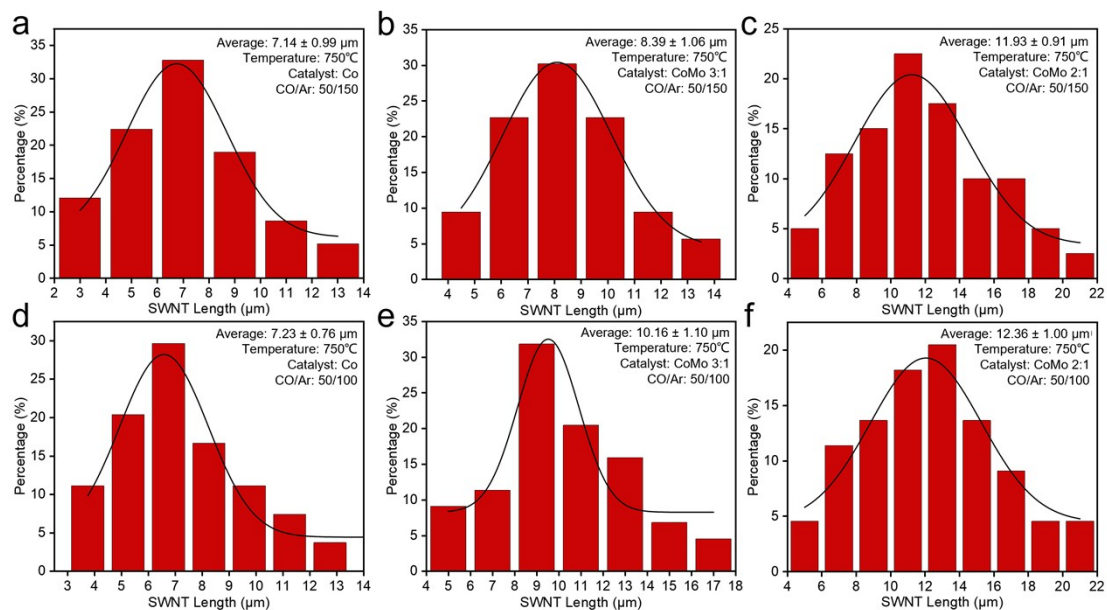


Figure S7. Length distributions of as-grown SWNTs at 750 °C under CO/Ar flow ratios of 50/150 and 50/100, grouped by catalytic active species, **(a, d)** Co, **(b, e)** Co/Mo 3:1 and **(c, f)** Co/Mo 2:1 respectively.

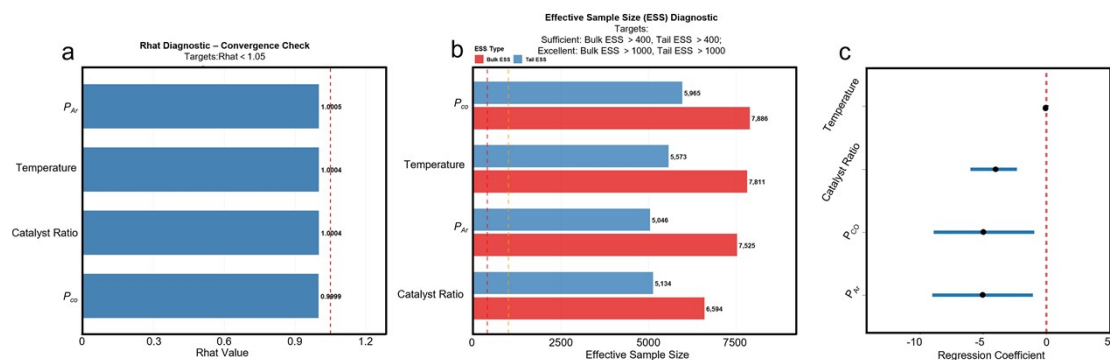


Figure S8. Validation of Bayesian logistic regression model of CO based SWNT growth process. (a) the Potential scale reduction factor (\hat{R}) value of variables and (b) Effective sample size of each variable. (c) correlation regression coefficient of different variables of SWNT growth result, using CO as carbon source. P_{CO} and P_{Ar} indicates the percentage of CO and Ar in total gas flow respectively, as the CO flow rate is fixed at 50 sccm. The 95% confidence intervals of the variables are: Temperature (-0.00054 ± 0.0001), Catalyst Ratio (-4.03 ± 0.94), P_{CO} (-4.94 ± 1.99) and P_{Ar} (-5.03 ± 2.00).

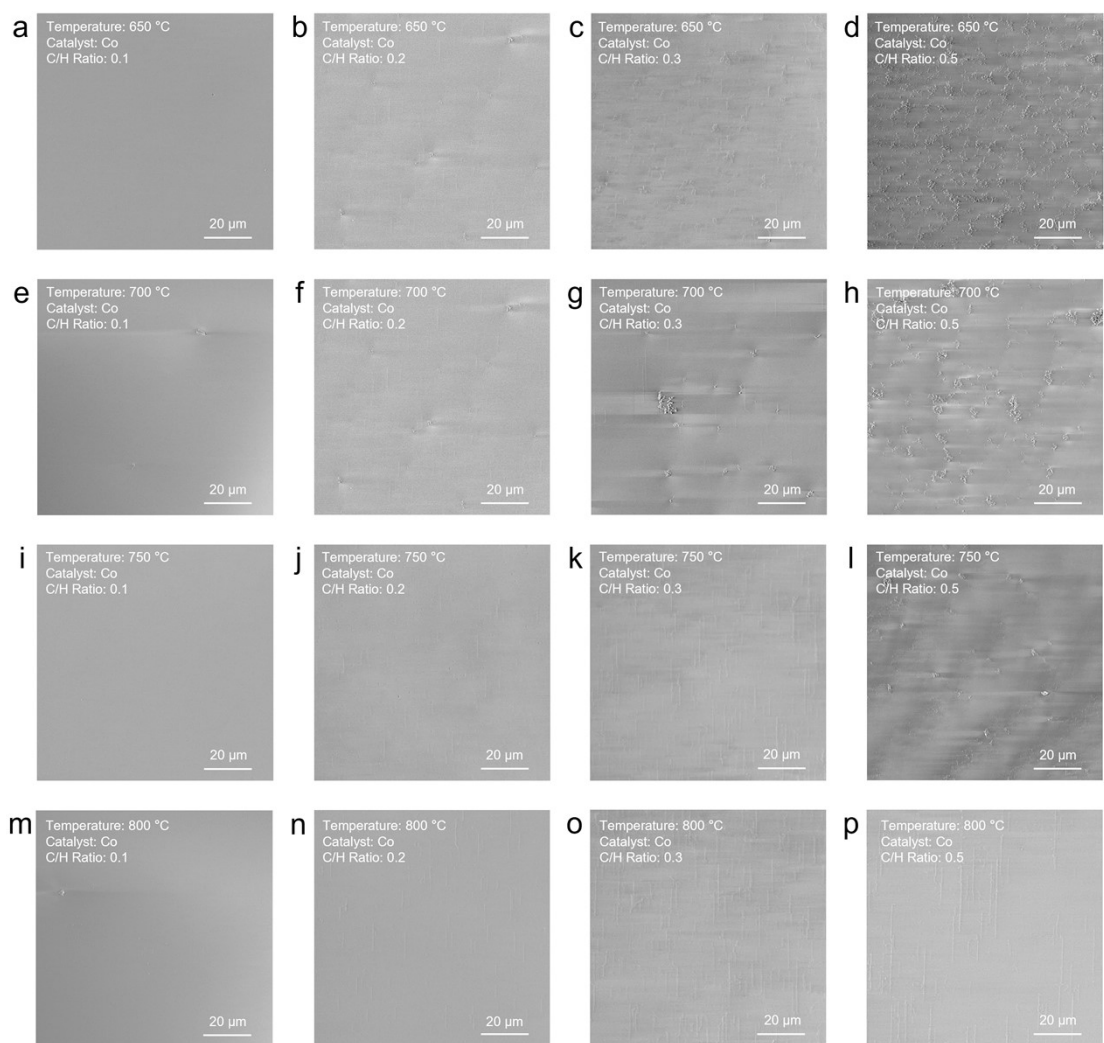


Figure S9. SEM images of quartz substrates loaded with Co catalyst after SWNT growth atmospheres with varied C/H ratios, performed at different growth temperatures, (a-d) 650 °C, (e-h) 700 °C, (i-l) 750 °C and (m-p) 800 °C respectively.

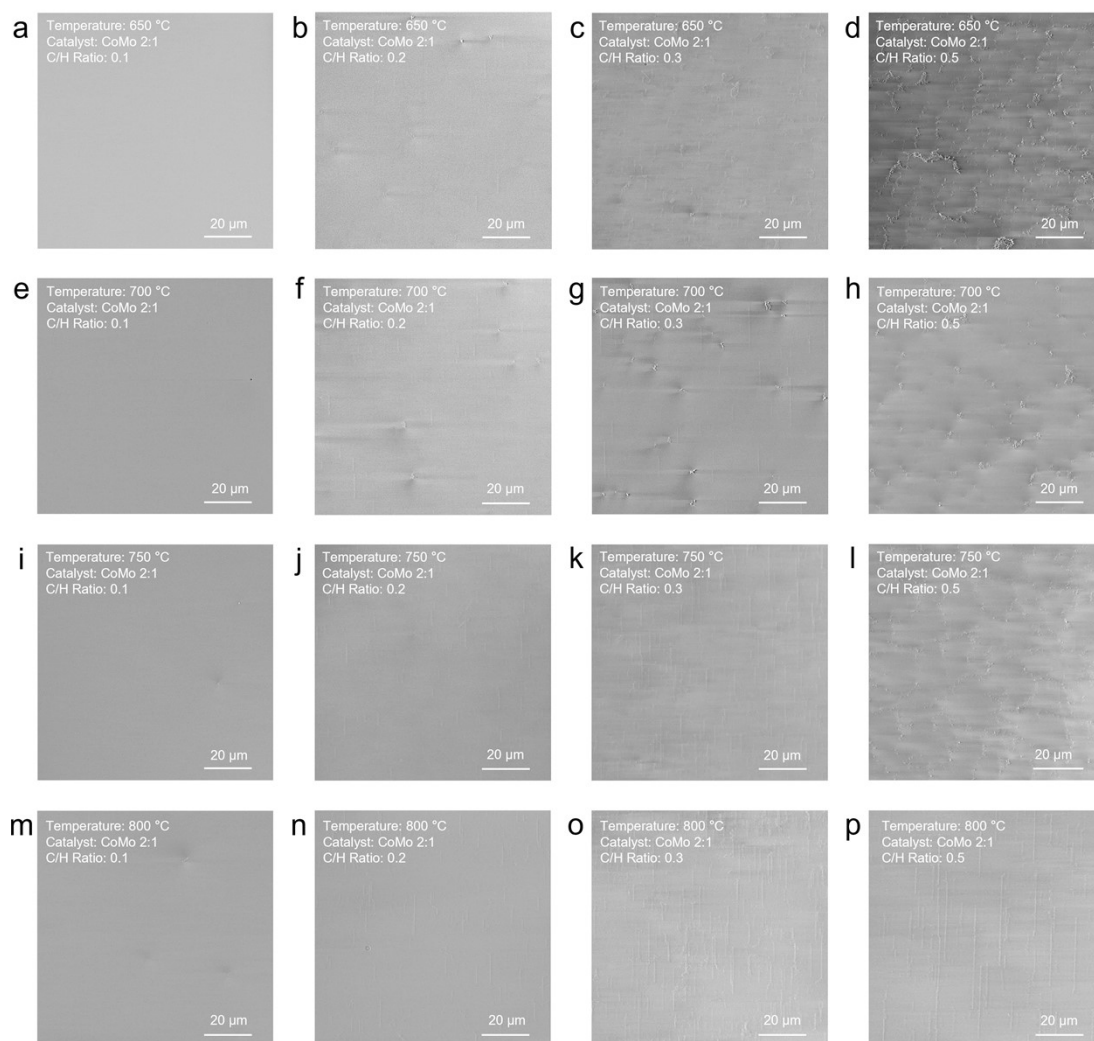


Figure S10. SEM images of quartz substrates loaded with Co/Mo (2:1) catalyst after SWNT growth atmospheres with varied C/H ratios, performed at different growth temperatures, **(a-d)** 650 °C, **(e-h)** 700 °C, **(i-l)** 750 °C and **(m-p)** 800 °C respectively.

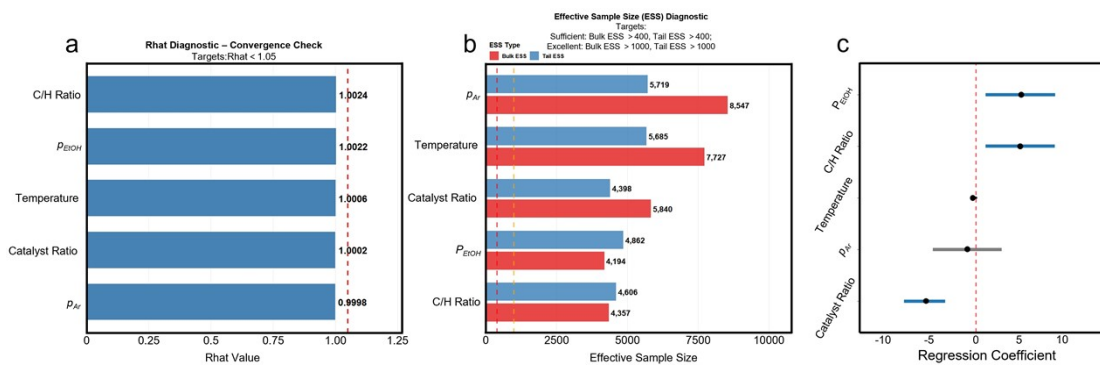


Figure S11. Validation of Bayesian logistic regression model of ethanol based SWNT growth process. **(a)** the Potential scale reduction factor (R) value of variables and **(b)** Effective sample size of each variable. **(c)** correlation regression coefficient of different variables of SWNT growth result, using ethanol as carbon source. P_{EtOH} and P_{Ar} indicates the percentage of EtOH and Ar in total gas flow respectively in **(c)**, as both Ar and H_2 flow rate is fixed at 200 sccm. The 95% confidence intervals of the variables are: P_{EtOH} (5.79 ± 3.80), C/H Ratio (4.98 ± 3.84), Temperature (-0.01 ± 0.003), P_{Ar} (-1.51 ± 3.83) and Catalyst Ratio (-5.64 ± 2.01).

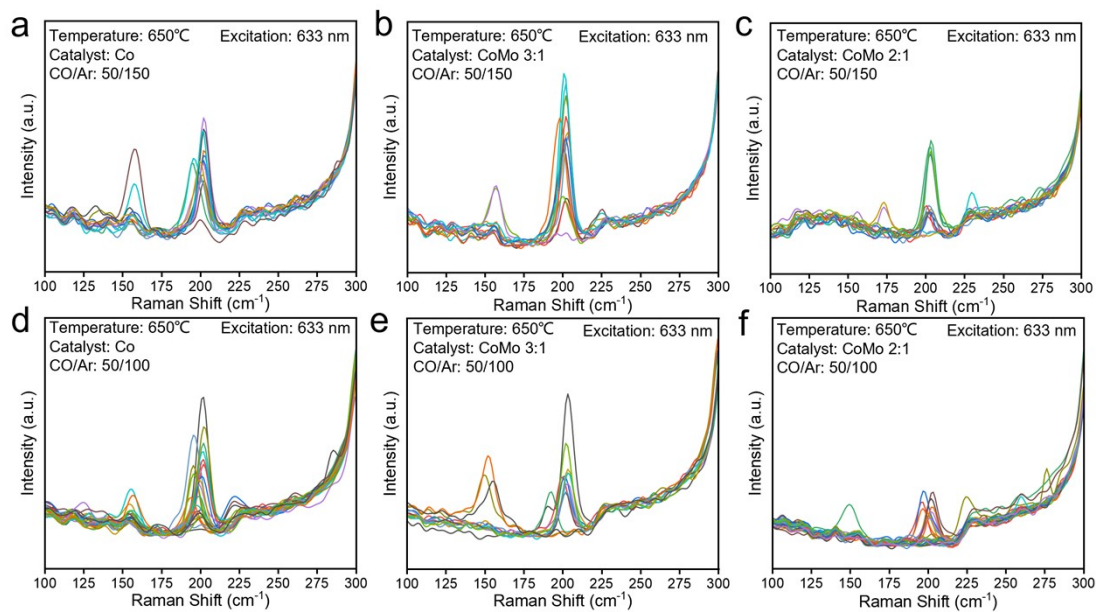


Figure S12. Raman spectra (532 nm laser excitation) of SWNT arrays grown from (a, d) Co, (b, e) Co/Mo 3:1 and (c, f) Co/Mo 2:1 catalysts at 650 °C, using CO (50 sccm) as carbon source with Ar flow rate of 150 and 100, respectively.

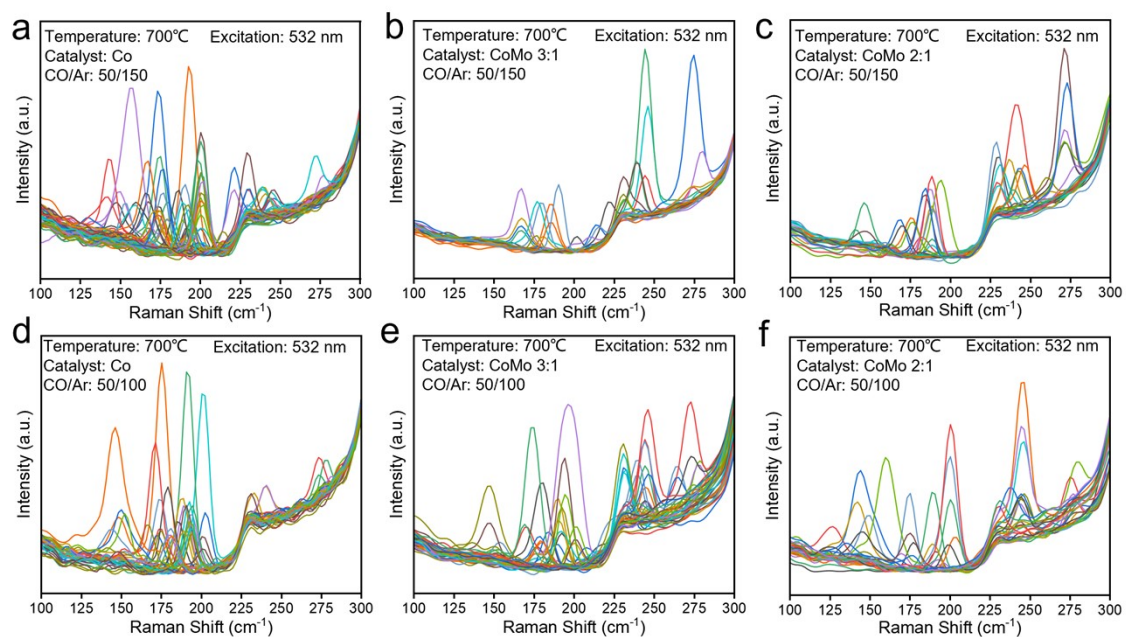


Figure S13. Raman spectra (532 nm laser excitation) of SWNT arrays grown from (a, d) Co, (b, e) Co/Mo 3:1 and (c, f) Co/Mo 2:1 catalysts at 700 °C, using CO (50 sccm) as carbon source with Ar flow rate of 150 and 100, respectively.

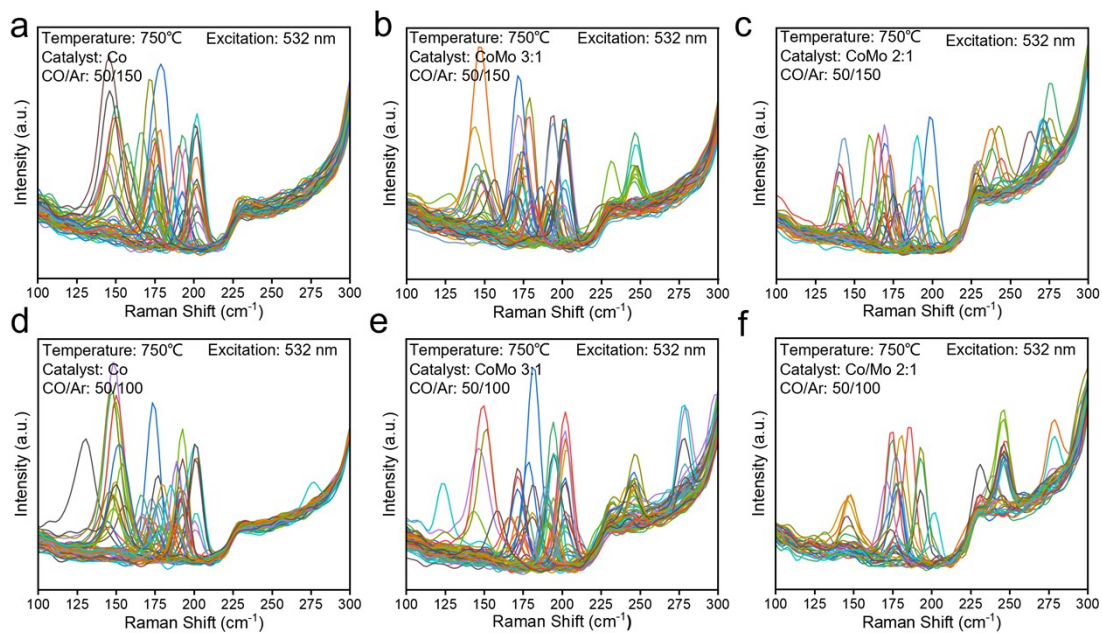


Figure S14. Raman spectra (532 nm laser excitation) of SWNT arrays grown from (a, d) Co, (b, e) Co/Mo 3:1 and (c, f) Co/Mo 2:1 catalysts at 750 °C, using CO (50 sccm) as carbon source with Ar flow rate of 150 and 100, respectively.

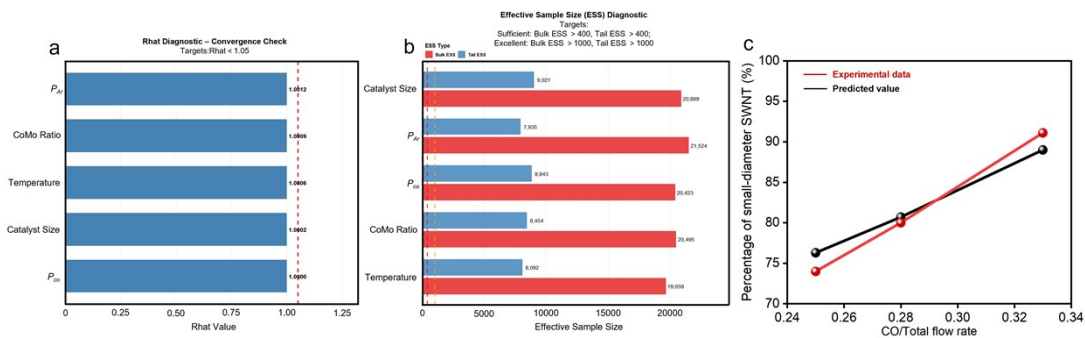


Figure S15. Validation of Bayesian model for small-diameter selectivity of SWNT arrays using CO as carbon source. (a) the Potential scale reduction factor (R) value of variables and (b) Effective sample size of each variable. (c) the small-diameter SWNT enrichment statistics of predicted data and experimental data under different P_{CO} by CoMo catalyst ratio of 1:1 at 650 °C. P_{CO} indicates the CO percentage in total gas flow in (c), as the CO flow rate is fixed at 50 sccm.

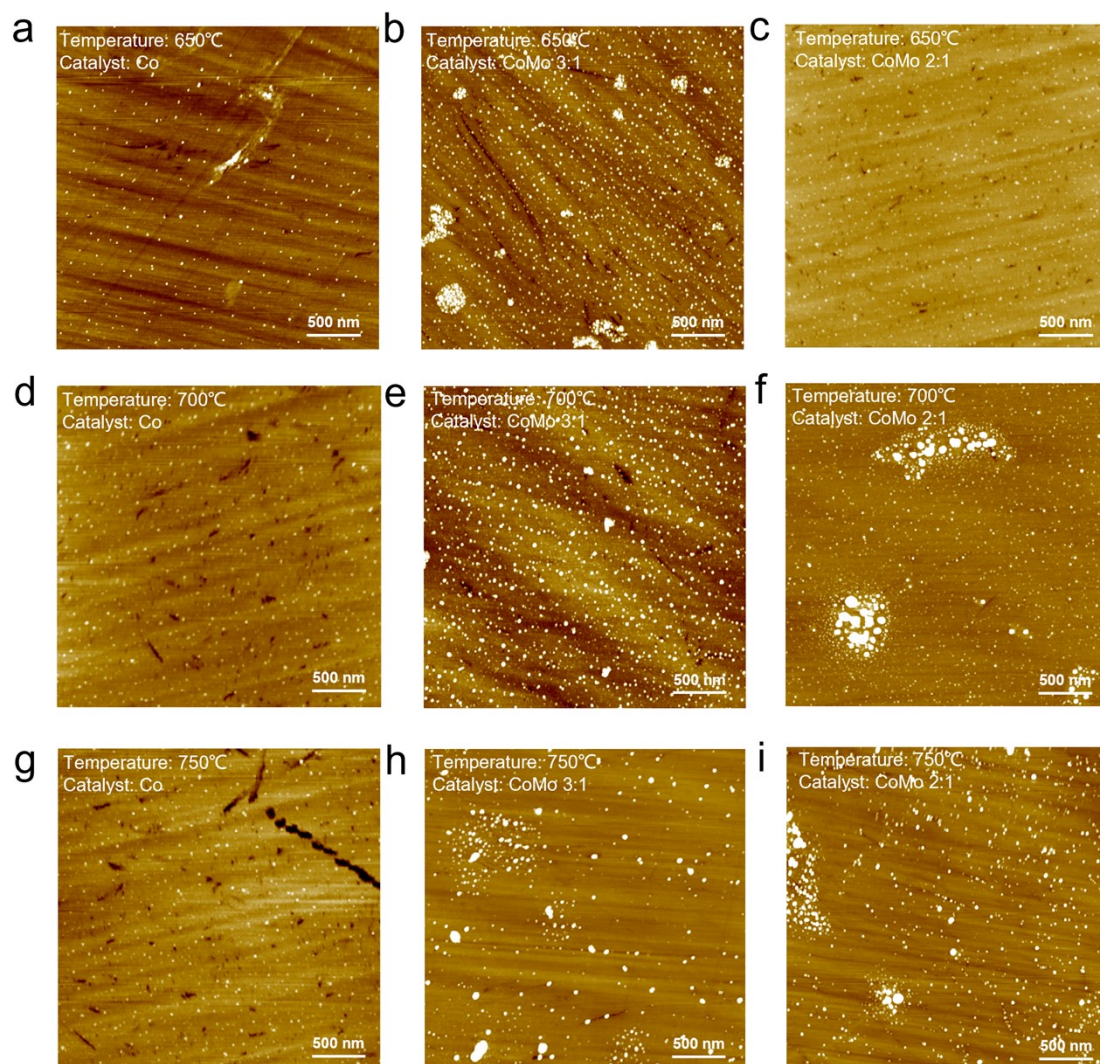


Figure S16. AFM images of Co/Mo alloy catalysts with different composition ratios supported on quartz substrates after 30 min of reduction at 500 °C, followed by 15 min annealing under Ar at different growth temperatures, (**a-c**) 650 °C, (**d-f**) 700 °C and (**g-i**) 750 °C.

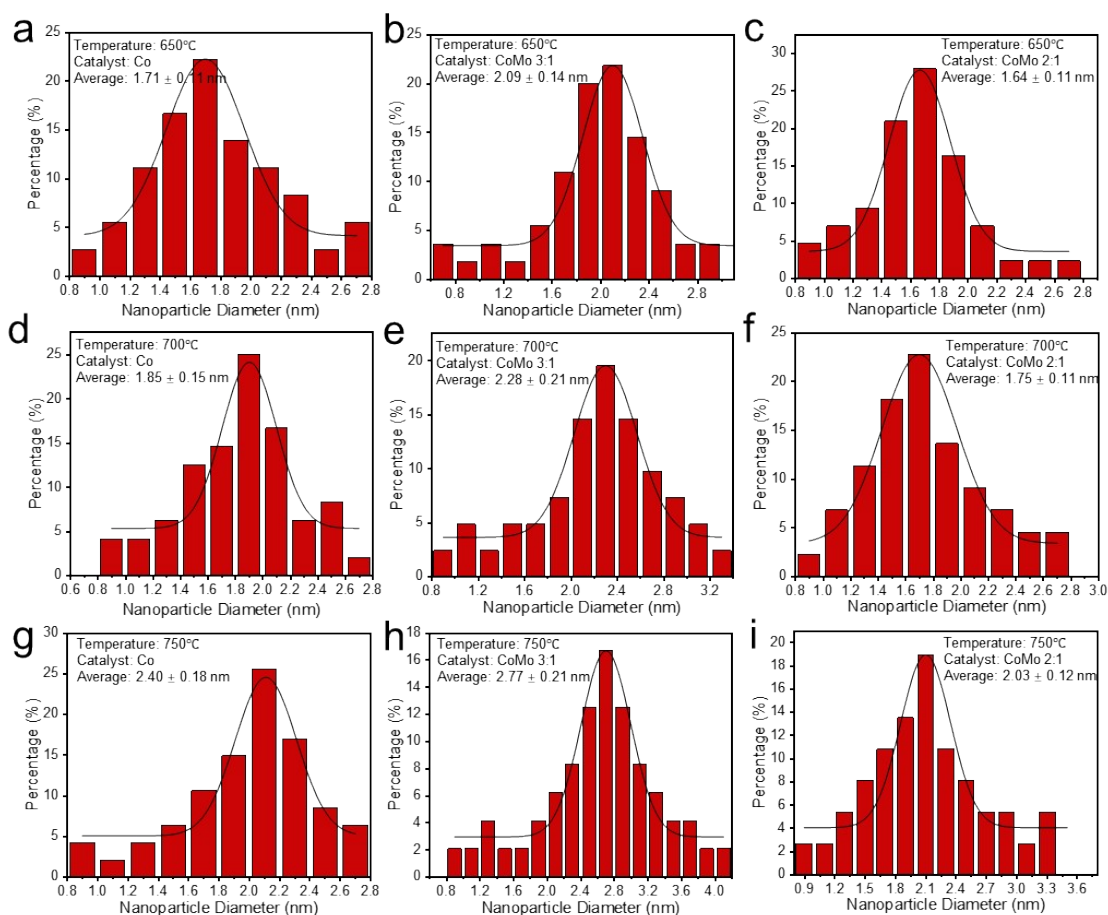


Figure S17. Nanoparticle size distribution of Co/Mo alloy catalysts with different composition ratios supported on quartz substrates after 30 min of reduction at 500 °C, followed by 15 min annealing under Ar at different growth temperatures, (a-c) 650 °C, (d-f) 700 °C and (g-i) 750 °C.

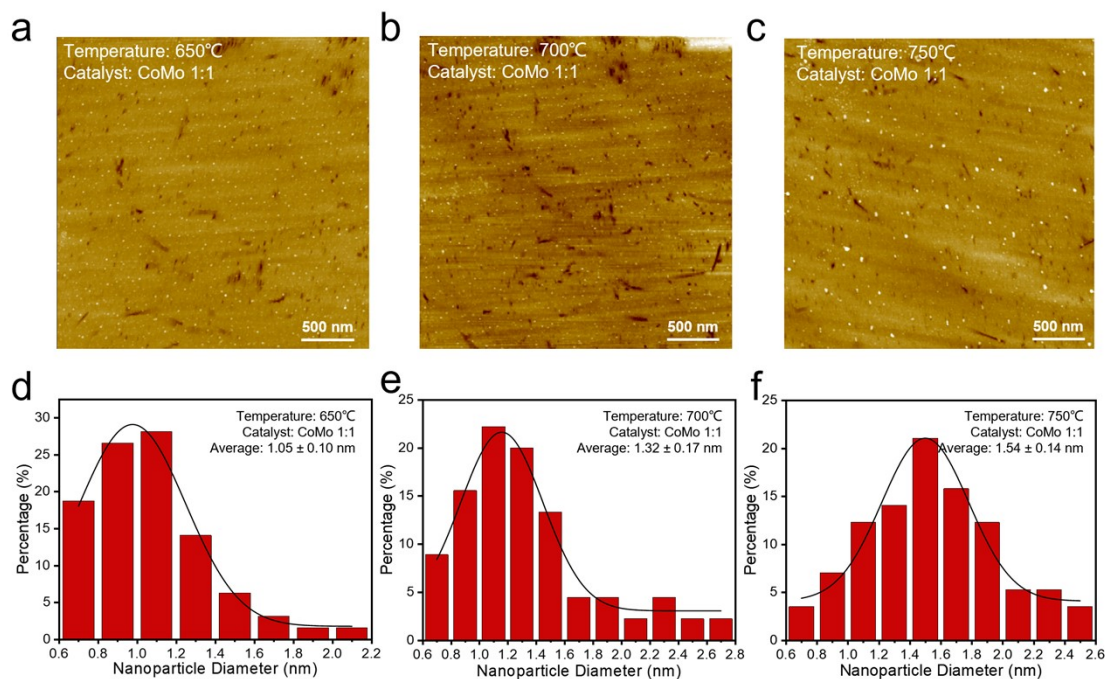


Figure S18. a-c, AFM images of Co/Mo (1:1) catalysts supported on quartz substrates after 30 min of reduction at 500 °C, followed by 15 min annealing under Ar at different temperatures, (a) 650 °C, (b) 700 °C and (c) 750 °C. d-f, Corresponding size statistics on catalyst acquired in a-c, (d) 650 °C, (e) 700 °C, (f) 750 °C.

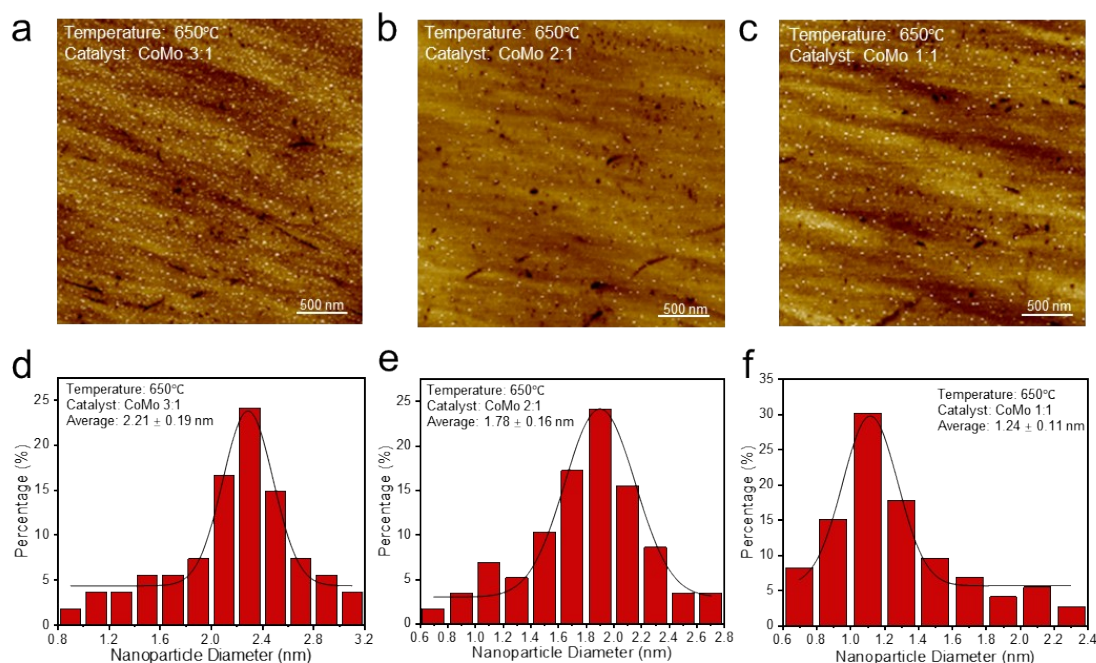


Figure S19. Characterizations of CoMo alloy catalysts after reduction at 650 °C with extra 15 min under the mixed Ar (100 sccm) and H₂ (50 sccm). a-c, AFM images of CoMo alloy catalysts with different ratios after the same treatment, (a) 3:1, (b) 2:1 and (c) 1:1 respectively. d-f, Corresponding size statistics of CoMo alloy catalyst nanoparticles in (a-c), (d) 3:1, (e) 2:1 and (f) 1:1 respectively.

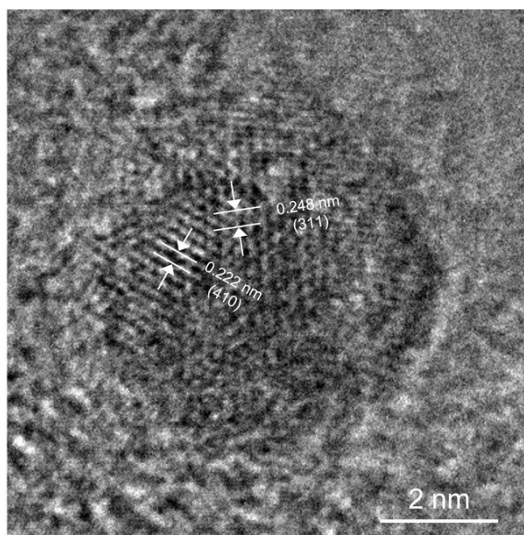


Figure S20. TEM image of Co₂Mo₃ alloy catalyst acquired at 650 °C through reducing the Co/Mo (1:1) precursor.

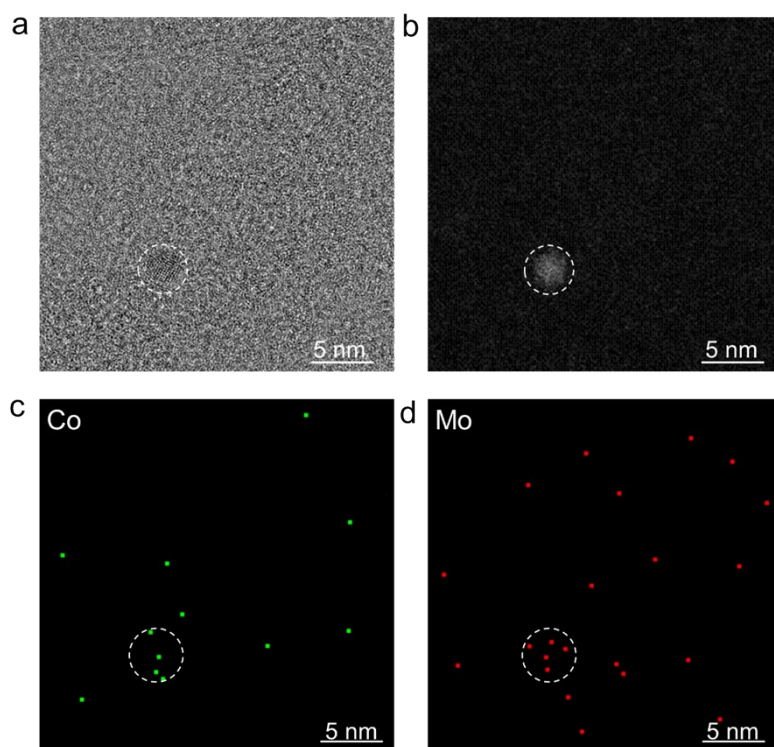


Figure S21. Energy-dispersive X-ray spectroscopy (EDS) elemental mapping of CoMo catalyst.

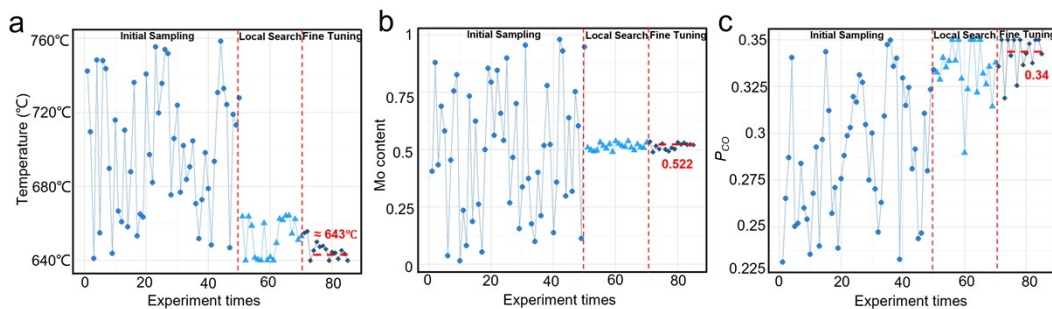


Figure S22. Iteration of (a) growth temperature, (b) Mo content and (c) P_{CO} in the progress of the Bayesian model to give the optimized experiment parameters. Mo content indicates the Mo molar ratio of the catalyst, as Co is fixed at 0.05 mM/L, and 0.522 means CoMo ratio close to 1:1 in (b). P_{CO} indicates the CO percentage in total gas flow, as the CO flow rate is fixed at 50 sccm, and 0.34 means CO/Ar flow ratio close to 50/100 in (c). The blue circles represent the initial data points, the light blue triangles are the local exploration points, and the dark blue squares are the subsequent experimental points suggested by the algorithm. The red dotted lines indicate the optimal values of each parameter.

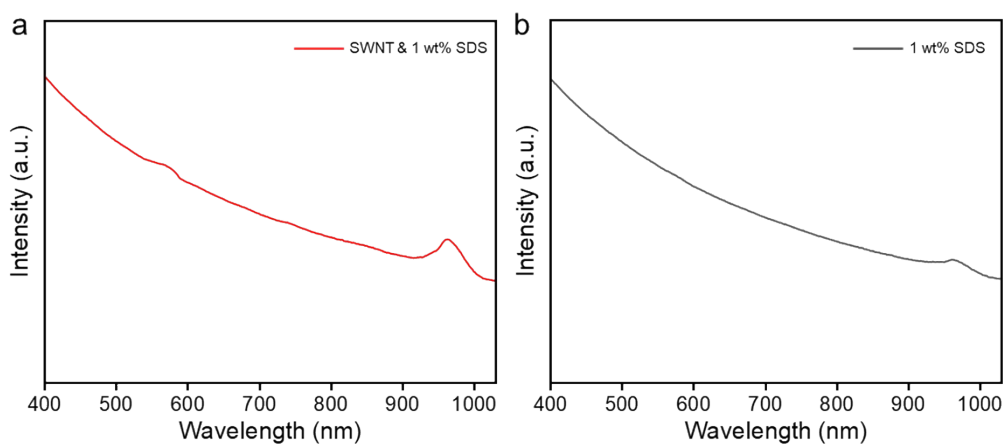


Figure S23. Original UV-vis-NIR absorption spectra of SWNT array dispersed in SDS solution (a) and of the blank SDS solution (b).